Soft Matter

PAPER

Torsion and curvature of FtsZ filaments†

Pablo González de Prado Salas,[a] Ines Hörger,[a] Fernando Martín-García,[bc] Jesús Mendieta,[bc] Álvaro Alonso,[e] Mario Encinar,[d] Paulino Gómez-Puertas,[b] Marisela Vélez*[ef] and Pedro Tarazona[g]

FtsZ filaments participate in bacterial cell division, but it is still not clear how their dynamic polymerization and shape exert force on the underlying membrane. We present a theoretical description of individual filaments that incorporates information from molecular dynamic simulations. The structure of the crystallized *Methanococcus jannaschii* FtsZ dimer was used to model a FtsZ pentamer that showed a curvature and a twist. The estimated bending and torsion angles between monomers and their fluctuations were included in the theoretical description. The MD data also permitted positioning the curvature with respect to the protein coordinates and allowed us to explore the effect of the relative orientation of the preferred curvature with respect to the surface plane. We find that maximum tension is attained when filaments are firmly attached and oriented with their curvature perpendicular to the surface and that the twist serves as a valve to release or to tighten the tension exerted by the curved filaments on the membrane. The theoretical model also shows that the presence of torsion can explain the shape distribution of short filaments observed by Atomic Force Microscopy in previously published experiments. New experiments with FtsZ covalently attached to lipid membranes show that the filament on-plane curvature depends on lipid head charge, confirming the predicted monomer orientation effects. This new model underlines the fact that the combination of the three elements, filament curvature, twist and the strength and orientation of its surface attachment, can modulate the force exerted on the membrane during cell division.

Introduction

FtsZ filaments play a central role in bacterial cell division.[1–3] They assemble into a ring in the midcell region and participate in the recruitment of other proteins forming the septal ring that exerts the force to divide the cell. The protein assembles *in vitro* in the presence of GTP[4] forming a large variety of dynamic structures depending on the pH, the presence of various monovalent salts, crowding agents and polycations.[5]

aDepartamento de Física Teórica de la Materia Condensada, Universidad Autónoma de Madrid, E-28049 Madrid, Spain

bCentro de Biología Molecular Severo Ochoa (CSIC-UAM), C/ Nicolás Cabrera, 1, Cantoblanco, 28049 Madrid, Spain

cBiomol-Informatics SL, Parque Científico de Madrid, C/ Faraday, 7, Cantoblanco, 28049 Madrid, Spain

dInstituto de Microelectrónica de Madrid, CSIC, Isaac Newton 8 (PTM), Tres Cantos, 28760 Madrid, Spain

eInstituto de Catálisis y Petroleoquímica, CSIC. c/ Marie Curie, 2; Cantoblanco, 28049, Madrid, Spain. E-mail: marisela.velez@icp.csic.es

fInstituto Madrileño de Estudios Avanzados en Nanociencia (IMDEA-Nanociencia)c/ Faraday 9, Cantoblanco 28049, Madrid, Spain

gCondensed Matter Physics Center (IFIMAC) and Instituto de Ciencia de Materiales Nicolás Cabrera, Universidad Autónoma de Madrid, E-28049, Spain

† Electronic supplementary information (ESI) available. See DOI: 10.1039/c3sm52516c

Supramolecular structures formed *in vitro* include two-dimensional rings, three-dimensional toroids and multistranded helices. Helical forms have also been observed *in vivo* by fluorescence microscopy in bacteria.[6,7]

Filament curvature is relevant for the formation of the Z-ring inside the cell and is also believed to play a central role in the force generation mechanism. Most theoretical models that describe force generation include curvature as an essential element and consider that a constriction force is generated by a switch from a straight to a curved filament conformation induced by GTP hydrolysis.[8–12] However, strong experimental evidence to support this nucleotide dependent conformational switch is lacking. Crystal structures of FtsZ containing different nucleotides revealed notably few differences between GTP and GDP containing monomers[13] and single filament dynamic behavior showed that the GTP hydrolysis rate is associated with the depolymerization velocity but not with the filament curvature.[14]

In spite of the fact that inside the cell filaments are attached to the membrane,[15] the effect of surfaces in modulating filament shape and curvature has not been sufficiently addressed. Recent experiments in Giant Unilamellar Vesicles (GUVs) showed that protein filaments artificially attached to the surface deformed the membranes inwards or outwards depending on the orientation of the filament binding.[16,17] More recent results examining the structure of the same artificially membrane

attached filaments on supported membranes with different curvatures have indicated that a filament twist, additional to the curvature, is needed to explain the observations.[18] Filaments formed directly on flat surfaces and characterized by AFM show that straight and curved filaments can coexist, depending either on the length of the filaments[19] or on the type of attachment to the surface.[20] All these results suggest that filament anchoring is important for determining their curvature and the way they deform the membrane.

In this paper we propose and test the hypothesis that considering both a preferred curvature and a twist in FtsZ filaments is enough to explain the formation of straight and curved filaments on flat surfaces. We show first that Molecular Dynamics (MD) simulations, based on the structure of the crystallized protein, show the presence of preferred curvature and torsion angles between neighboring monomers. We then use the bend and torsion angles and their fluctuations to develop a theoretical model to simulate the behavior of the twisted and curved filaments attached to surfaces. We find that orientation and attachment strength determine the shape of the filaments and the tension created on the surface. We finally analyse and explain existing results and show new experiments in which the structures formed by FtsZ oriented on lipid bilayers can be explained by the predictions made by the model.

The presence of a preferential filament curvature and torsion suggests a new way, independent of GTP hydrolysis, to control the tension generated on the membrane. For the right orientation, modulating attachment strength can induce a switch from a soft filament to a stiff off-plane curved filament that exerts a maximum force perpendicular to the surface.

Results

Twisted filaments: molecular dynamics simulations

The structure of the crystallized *Methanococcus jannaschii* FtsZ dimer[13] has been used to search the best possible superposition of the structure of one monomer on that of the other monomer. By this computational elongation, we have generated the polymer structure in Fig. 1 that shows a helical structure with the C-terminal end of the protein located in the same orientation each approximately 18 monomers (Fig. 1A). During unrestricted MD (see below), the helical structure exhibits a contraction–extension behavior; *e.g.*, after 8 ns of MD, the polymer showed the same orientation of the C-terminal end each 8–10 monomers (Fig 1B).

The MD simulations of an FtsZ pentamer were performed following the method previously published.[25] Using the complete modeled pentamer, unrestricted MD of 288 517 atoms, including water molecules in the solvent box, were carried using AMBER 12.[28] The sampling over 80.0 nanoseconds shows the fluctuations of the curvature angle between the mean directions of the three monomers at each end of the pentamer and the torsion angle (defined from the C-terminal end) (Fig. 2).

Theoretical model

Helical shape and fluctuations of a free FtsZ filament

The helical structure may be characterized by the mean angles observed in the MD simulation of the pentamer.

The structure of the FtsZ pentamer was explored along the molecular dynamic simulation for a total running time of 26.7 nanoseconds. Their statistical properties have been obtained neglecting the first 13.3 ns, to allow for the thermalization of the initial configuration. The bending of the FtsZ pentamer is measured by the angle α, calculated between the directions of the lines from the first to the third, and from the third to the fifth monomer, so that it accumulates the equivalent of the bending angles in two consecutive bonds $\alpha = \pi - \theta_1 - \theta_2$. The mean value was $\langle\theta\rangle \equiv \langle\theta_{1,2}\rangle \approx 7.6°$ between the directions of neighbor monomers (see the histogram of $(\pi - \alpha)/2$ in Fig. S1 in the ESI†). The observed fluctuations of α correspond to two consecutive bonds, that we take as independent from each other $(\langle\theta_1\theta_2\rangle = \langle\theta_1\rangle\langle\theta_2\rangle)$, so that $\Delta\alpha \equiv \sqrt{\langle\alpha^2\rangle - \langle\alpha\rangle^2} \approx 3.4°$ corresponds to $\Delta\theta \equiv \sqrt{\langle\theta^2\rangle - \langle\theta\rangle^2} = \Delta\alpha/\sqrt{2} \approx 2.4°$. The angle δ
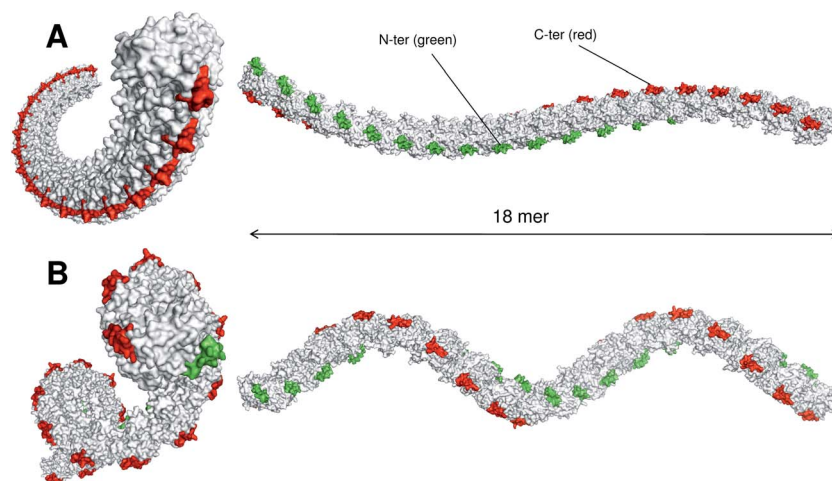

Fig. 1 Structural models for FtsZ polymers in solution. (A) Longitudinal elongation of the crystallized structure of FtsZ dimer.[13] Residues located at the N-ter (green) and C-ter (red) ends of the crystal structure are highlighted. (B) Longitudinal elongation of a short FtsZ polymer[24] after 8 nanoseconds of unrestricted molecular dynamics.

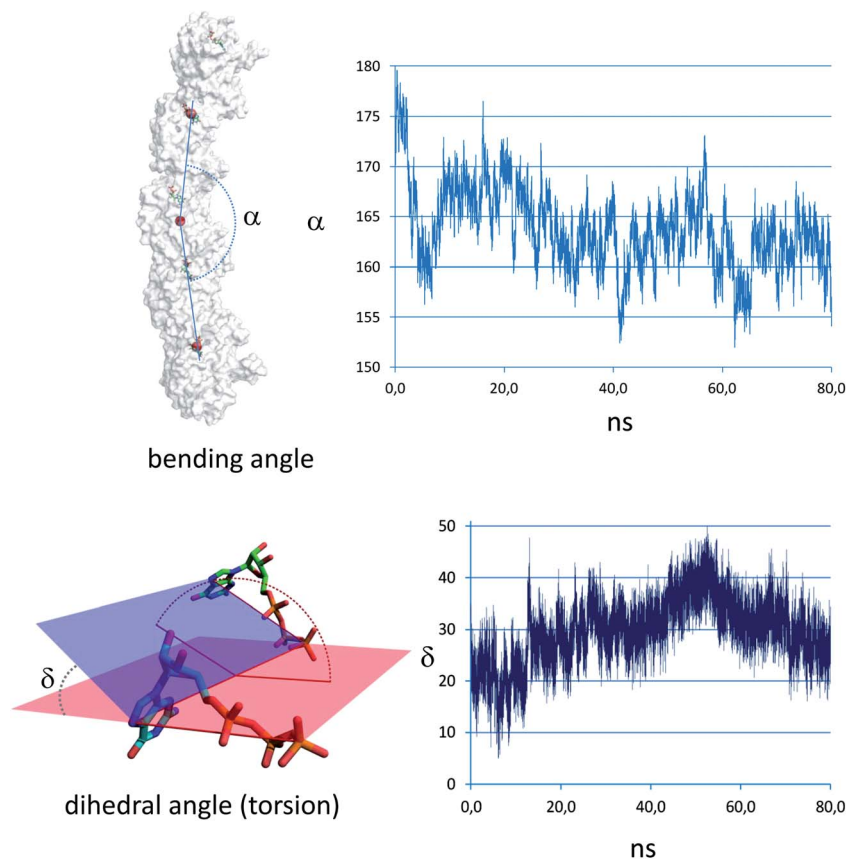Labels in figure: N-ter (green), C-ter (red), 18 mer, A, B

Fig. 2 Fluctuations on the curvature and torsion angles during 80 ns of unrestricted molecular dynamics. Bending angle α was measured using as references the center of masses for the third monomer and the position of the GTP molecules in the first and last interfaces. Torsion angle δ was measured using as references the position of atoms in the GTP molecule, as indicated in the lower left diagram.

measures the orientation mismatch between two consecutive monomers with respect to the axis joining their bonding sites. We find $\langle\delta\rangle \approx 20°$, and $\Delta\delta \equiv \sqrt{\langle\delta^2\rangle - \langle\delta\rangle^2} \approx 4°$ (see also the histogram in Fig S1†). These mean values and mean fluctuations may be taken with a confidence of about $\pm0.5°$, from the possible changes if we analyse the simulation results over time intervals with ±1 nanoseconds.

The local tangent plane is approximately that containing the C-terminal groups on the outer side and the N-terminal groups on the inner side of the curved polymer.

The angular fluctuations observed in the MD simulation of the pentamer may be used to estimate the flexibility of the filaments. Assuming that the MD run is a good sample of thermal equilibrium, the elastic constants that describe the bending and the torsion of the filament, $\kappa_\theta = kT/\Delta\theta^2$ and $\kappa_\delta = kT/\Delta\delta^2$ can be used to describe the increase in the free energy per bond due to the elastic energy needed to reorient the monomers.

$$U = -U_{\rm b} + \sum_{i=1}^{N} \left[\frac{\kappa_\theta}{2}(\theta_i - \langle\theta\rangle)^2 + \frac{\kappa_\delta}{2}(\delta_i - \langle\delta\rangle)^2 \right], \qquad (1)$$

where $U_{\rm b}$ is the bond free energy in the optimal (helical) structure. The estimated values $\beta\kappa_\theta \approx 583$ and $\beta\kappa_\delta \approx 200$ indicate that filament torsion is about three times more flexible

than filament bending. The persistence length for the helical axis of a free filament, with these elastic constants, would be about 4 μm (i.e. above one thousand monomers), which is consistent with some previously estimated values,[29] but larger than other estimations. The determined value is likely to be conditioned by the experimental technique used to do the measurements. Results obtained from cryoelectron microscopy give a slightly smaller value, 1.5 ± 0.25 μm,[30] whereas the persistence length estimated from transmission electron microscopy images is only 180 nm.[31] It is possible that the negative stain used in the sample preparation for TEM can affect the rigidity and length of the filaments adsorbed on the carbon grid. (See ESI† Section 1 for a full description of the free FtsZ filaments.)

Model for elastic helical filaments anchored to a planar substrate

The shape and flexibility of the free FtsZ helical filament are affected when the protein is adsorbed on a planar substrate. We first consider the effect of the surface proximity on the properties of the filaments by restricting the bending and torsion angles between monomers without including any energetic contribution from monomer anchoring to the surface.
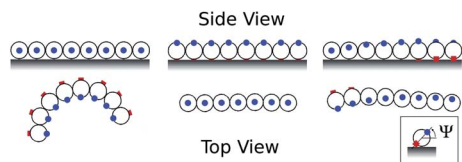
Fig. 3 Orientation of the filaments on surfaces. Red and blue dots indicate the position of the carboxy and amino termini of the protein. The angle ψ determining the orientation of the tangential plane of the free filament with respect to the surface is illustrated. $\psi = 0°$ on the first panel, with the tangential plane parallel to the surface. $\psi = 90°$ on the central panel and on the third panel, since the attachment is not fixed, ψ takes values from $0°$ to $90°$. Although not illustrated, ψ could vary from $0°$ to $360°$.

We define the angle ψ as the orientation of each monomer with respect to the surface (see Fig. 3). For small ψ_i values, the natural tangential plane of the free filament is nearly parallel to the substrate. The optimal on-plane angle and elastic bending constant κ_θ are the same as in the free helix (eqn (1)).

In the opposite limit, when $\psi_i \approx 90°$, the natural tangent plane of the free filament is perpendicular to the substrate, and there is no spontaneous curvature for the filaments on the surface. The free energy to keep the filaments straight is $\approx$ 3 kcal mol^{-1}, *i.e.* nearly 5 kT at room temperature, and therefore quite relevant to determine the preferential orientation and the on-plane curvature of filaments on planar substrates under experimental conditions. (See Section 2 in the ESI† for the full evaluation of the effect of the surface proximity on the torsion and curvature elastic constants.)

In addition to the energetic contribution due to the induced bending and torsion of the filament, we can also include the free energy due to the direct interaction of each FtsZ monomer with the surface $u_a(\psi)$. We then explore the thermal equilibrium distributions for filaments with the bending and torsional energy using a simple anchoring potential model,

$$u_a(\psi) = \min\left(0, -U_a + \frac{\kappa_\psi}{2}(\psi - \psi_o)^2\right), \quad (2)$$

with the minimum free energy $-U_a$ when the monomers have the orientation ψ_o, and with a monomer-surface binding stiffness controlled by κ_ψ. This term, added for all the monomers in a filament $\sum_i u(\psi_i)$, describes the specific anchoring of the protein monomers and depends on the nature of the substrate and the way the protein is attached to it. When added to the contribution from the geometrical constrain to force the free filament helix on the substrate plane described above, it provides the full description of filaments on a surface.

Simulations were done for ideal filaments, *i.e.* neglecting any interaction beyond the independent structure of each bond. The monomers were added one by one to the end of the chain with the orientations $\psi_i, \psi_{i+1}, \ldots$, chosen randomly to reproduce the equilibrium probability distribution in their torsional state. Long filaments, up to $N = 5000$ monomers, were simulated.

The sketches shown in Fig. 4 show typical filament shapes obtained for different ψ_o values and stiffness κ_ψ in the anchoring potential (eqn (2)). The observed shapes show that a
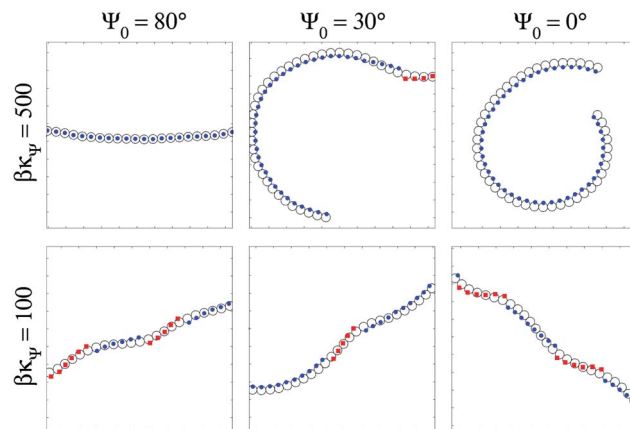

Fig. 4 Typical shapes of FtsZ filaments on a planar substrate, obtained from the independent bond distribution model, with the helix parameter and elastic constants obtained from the fluctuations of the free pentamer, under different parameters for the anchoring of the protein monomers on the substrate. ψ_o indicates the angle of the tangential plane with respect to the surface and $\beta\kappa$ indicates the strength of the attachment.

broad range of anchoring parameters lead to the formation of rings (or rolls with multiple rounds if the effects of the excluded area and the lateral attraction between the filaments were included).

The effect of specific anchoring may be found in the variation of the mean on-plane angle $\langle\theta_i\rangle = \langle\theta_M(\psi_i, \psi_{i+1})\rangle$, or equivalently in the optimal ring radius $\langle R\rangle = \sigma/\langle\theta\rangle$ for monomers of size σ. For very stiff anchoring, *i.e.* large κ_ψ in eqn (2), all the monomers would have similar orientation $\psi \approx \psi_o$ (see ESI†). When the optimal anchoring on the substrate keeps the orientations of the tangential plane in the free filament *i.e.* $\psi_o \approx 0$ the filaments would have their maximum curvature $\langle\theta\rangle \approx \theta_o$. Increasing ψ_o reduces the mean curvature, since the anchoring on the planar substrate forces the filament partially out of its spontaneous curvature as a free helix. For large enough values of ψ_o, the combined effect of the anchoring on the substrate and the spontaneous torsion along the filament lead to $\langle\theta\rangle = 0$, *i.e.* filaments without spontaneous on-plane curvature (Fig. 4 upper panel). For loose anchoring, low κ_ψ in eqn (2), the mean curvature of the filaments is always very small and changes very little with the value of ψ_o. The spontaneous torsion of the filament tends to keep the angle ψ_i changing along the filament and regions with $\psi_i \approx 0$ and others with $\psi_i \approx 180°$ cancel out the mean curvature (Fig. 4 lower panel)(see Section 3, ESI†).

Experimental verification

The theoretical model presented above, that relates the filament length, curvature and torsional strain, optimal anchoring and monomer orientation with the final conformation and shape fluctuations on a flat surface, can be used to describe the shape of FtsZ filaments on surfaces observed by AFM microscopy. This analysis provides an explanation to filament shapes in two sets of experimental observations: filaments adsorbed on mica, and
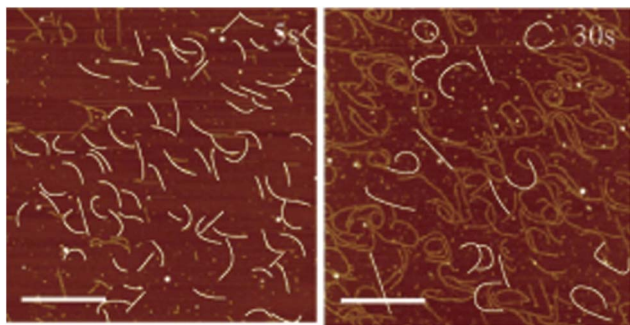
Fig. 5 Filaments formed on mica incubated during 5 s (left) and 30 s (right) with 80 nM FtsZ in polymerization buffer before drying the sample. Images were taken from ref. 19. The scale bar is 500 nm. The analyzed polymers are represented as white lines.

filaments anchored on lipid bilayers with a well defined orientation.

AFM on mica

When FtsZ filaments are absorbed on a mica surface there is no direct control over the orientation of the monomers on the surface. The measured height of the filaments indicates that they are in close contact with the planar substrate, but there is no information about monomer orientation and anchoring.

It was recently shown that a mica surface promotes the assembly of cytoskeletal proteins. FtsZ was able to polymerize directly on the surface when incubated below their critical concentration. Imaging was performed in air after fixing the sample with 0.02 (w/v) uranyl acetate[19] at different incubation times following the polymerization process. Longer incubation times gave long and curved filaments similar to ones previously observed under solution.[32,33] Short incubation times showed coexistence between very straight and curved filaments
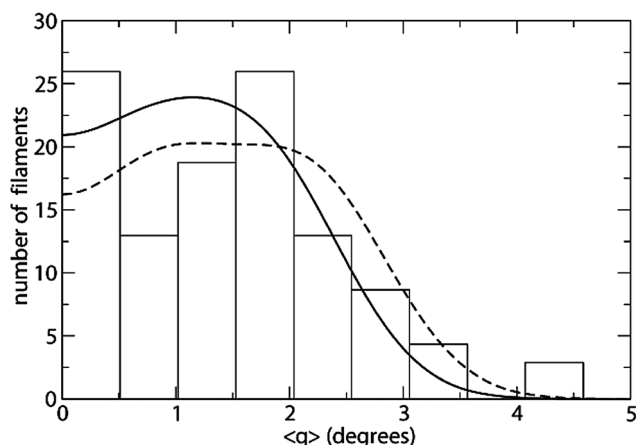

Fig. 6 Distribution of the number of selected filaments in Fig. 5, in terms of their mean curvature after 5 s incubation time. The lines represent the predictions of the physical pendulum model, described in Section 4 of the ESI,† for a mixed population of filaments in two local minima of the torsion-anchorage free energy. Solid line assumes a mean on-plane angle $\theta = 2°$, and the broken line $\theta = 2.4°$.

(see Fig. 5) and their angle distribution differed from the Gaussian distributions obtained when filaments were imaged under solution.[29]

Fig. 6 presents the histogram of mean curvatures extracted from the digitalized images. A possible explanation for the dimorphism of the filaments comes from the crossed effects of the internal torsion of the bond between protein monomers and the anchoring of each monomer to the surface.

The curvature-torsion model indicates that restricting the shape of the filaments to be adsorbed to a surface is energetically unfavorable. Depending on the filament length, this energy cost could be compensated by the energy gained by the anchoring. This hypothesis leads to a discrete set of separate twist structures, as local minima of the torsion plus anchoring energies, so that the filament may be trapped in a sub-optimal structure for a long time, before the thermal fluctuations take it over the energy barriers towards the global minimum energy structure (Section 4 in the ESI†).

The observed polymorphism of the filament shapes in the AFM images could therefore represent the coexistence of filaments in different twist configurations: short filaments remain twisted and are therefore straight, whereas for longer filaments, the interaction energy between monomers and the substrate is strong enough to overcome the cost of untwisting and the filaments adopt curved shapes.

The spontaneous curvatures observed experimentally are compatible with $30° \leq \psi_o \leq 45°$, indicating that the C-terminal to N-terminal plane is standing at such angles with respect to the mica plane.

Filaments oriented on lipid surfaces

In order to further test the hypothesis that the orientation of the tangent plane of the filaments with respect to the surface determines the curvature, we performed experiments anchoring a mutant form of *E. coli* FtsZ containing a cysteine in position 255 to lipid surfaces. FtsZ monomers covalently attached to a lipid surface through a well defined position can reversibly polymerize on the surface in the presence of GTP.[22] If the cysteine is located near the C terminal region of the protein, anchoring to the lipid bilayer would leave the C-terminal to N-terminal plane perpendicular to the surface, making $\psi_o \approx 90°$ and giving rise to straight filaments (Fig. 7A).

Fig. 7B shows the straight filaments observed on lipid bilayers containing a zwitterionic lipid head (DOPC). However, when the same proteins are attached to lipids containing a negatively charged head (cardiolipin), filaments are curved (Fig. 7C). Since the cysteine is located near the carboxy terminal end but surrounded by a patch of negatively charged lipids (see Fig. S6 in ESI†), we interpret this result as indicating that the surface negative charge reorients the C-terminal N-terminal plane with respect to the plane of the membrane, leaving it close to the previously estimated value for the mica, also negatively charged, of $30° \leq \psi_o \leq 45°$. Although the attachment of the protein to the lipid is made through a covalent bond, the S9 loop region where the cysteine is located has been defined as
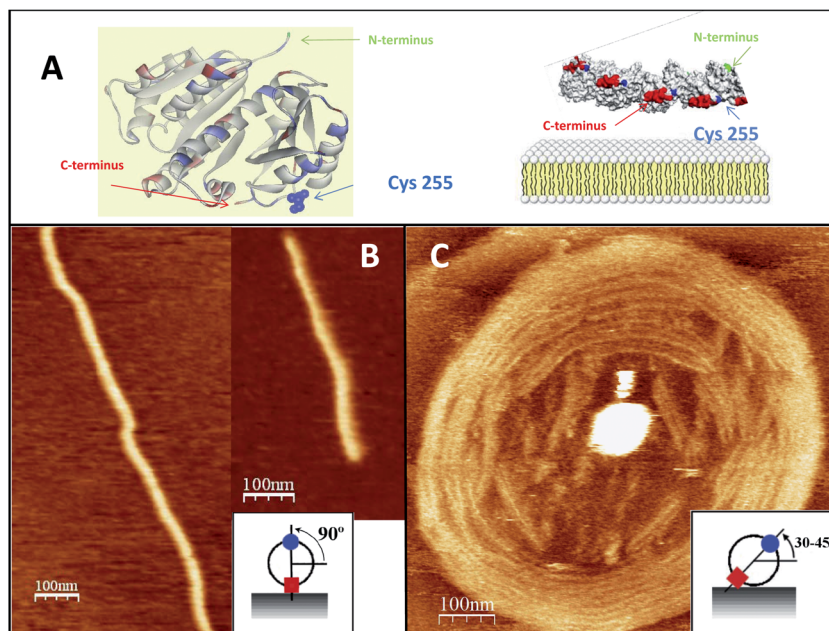
Fig. 7   FtsZ covalently anchored to lipids. (A) shows the position of the cysteine used to anchor the protein, located near the C terminus end. The C−N tangent plane of the untwisted filament stands at ≈90° with respect to the surface. (B) Straight filaments on a neutrally charged lipid surface. (C) Curved filaments on a negatively charged lipid surface.

being highly flexible,[34,35] allowing for reorientation of the tangential torsion plane with respect to the surface. Curved filaments were also observed on lipid bilayers of different compositions containing negatively charged *E. coli* polar lipids (Fig. S7†).

Discussion

This is not the first time that a twist in FtsZ filaments is suggested. Theoretical models,[37,38] molecular dynamic simulations[39] and, more recently, experimental observations[18] have considered the existence of a twist angle between the monomers constituting FtsZ filaments.

In the first case, the authors suggested that the formation of coils or rings from different cytoskeletal proteins observed inside bacteria could arise, at least in part, from the interaction of the inherent mechanical properties of the protein polymers and the constraints imposed by the curved cell membrane. The polymer model used included all turning angles of the membrane bound monomers: left-right, up-down and a rotation around the polymer axis.[37]

Recent molecular dynamics simulations[39] directed towards understanding the role of the phosphorylation state of the nucleotide within the monomers on the filament curvature also found that both GDP and GTP containing monomers presented a twist angle. Those simulations were performed using a modelled FtsZ dimer and extrapolating their findings to polymers, instead of the use of modelled oligomer-pentamer as in the present work. In addition, the authors concentrated mainly in interpreting the bending motion between monomers and disregarded the importance of the twist angles.

Very recently, elegant experiments using curved biomimetic platforms showed that FtsZ containing a membrane targeting sequence (MTS-FtsZ) formed filaments that wrapped around glass cylinders. The angles formed between the filaments and the cylinder axis differed from expected for filaments having only a spontaneous curvature.[18] Including both an intrinsic curvature and a spontaneous twist in the theoretical model of a helical filament bound to a curved surface could however explain the experimental results.

The work presented here builds the theoretical model including both the bend and twist angles between protein monomers that define the FtsZ pentamer obtained from MD simulations. Such a theoretical description of the shape and fluctuations of free filaments has at least two important advantages over previously published models:[18,37] (1) the quantitative estimate of the bending and twisting rigidities are reliable, as confirmed by their agreement with experimentally estimated values of the persistence length[29,30] and (2) the angles and their fluctuations are very well defined in space with respect to the protein coordinates. These two elements allow us to obtain additional information: how the orientation of the protein monomers affects the overall filament shape and how the anchoring strength can modulate both their shape and properties.

We can now address a very relevant biological question: the relationship between filament curvature and the orientation of the monomers on the surface. It is known that both FtsA and ZipA, proteins that link FtsZ to the membrane, bind to the carboxy terminus end of the protein.[15] Our model indicates that this orientation has important consequences: it allows for the formation of straight filaments with $\psi_o \approx 90°$ that, depending on the tightness of the bonding, could transmit the tension to the underlying surface.

Force on the substrate

We can estimate how protein orientation and attachment strength affect the stress exerted on the substrate. The maximum force would be done when the preferential anchoring of the filament sets the tangent plane perpendicular to the substrate, $\psi_o \approx \pm 90°$, and it would vanish when the filament shows the maximum on-plane curvature with the tangent plane parallel to the substrate, $\psi_o \approx 0$ or $180°$. Our analysis also indicates that the presence of a twist can be used to modulate that force depending on the tightness of the anchoring. A loose attachment of the monomers to the surface allows releasing the filament bending strain, whereas a very tight anchoring generates extremely rigid filaments that can produce the maximum stress on the substrate. The soft twist provides a valve to release the tension created by the oriented attachment as long as the link is flexible. In contrast, a stiff attachment would cancel this effect and allow the filaments to display the full potential of their geometrical and mechanical design to generate force: presence of stiff filaments with a curvature perpendicular to the plane of the membrane. The possibility that twist, curvature, orientation and attachment of the filament with respect to the membrane participate in modulating the force offers possible explanations to the role played by different proteins that bundle the filaments and attach them to the surface.

Fig. 8 shows, for filaments with the bending rigidity extracted from the MD simulation of the FtsZ pentamer, the force per protein monomer produced over a broad range of anchoring angles, from $40° \leq \psi_o \leq 130°$. The amount of force exerted by the filaments on a curved surface is proportional to the mismatch between the spontaneous curvature of the filaments and that of the surface. The force decreases as the substrate curvature approaches that of the free filament. Fig. 8 shows the force estimate for several values of surface curvature, from a flat surface to 74 nm in diameter (about one seventh the diameter of an E. Coli bacteria).

On an elastic substrate like a free standing lipid bilayer, the filaments would deform the membrane inducing the curvature needed to compensate for its spontaneous off-plane curvature. This has been observed experimentally.[17] Estimates of the required radial force to produce the observed deformations of
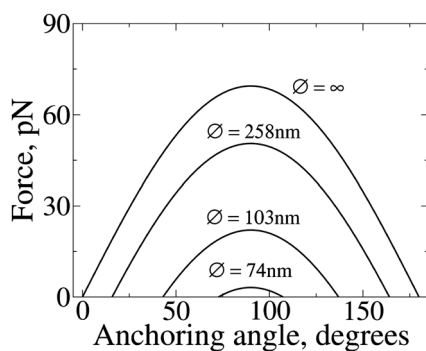

Fig. 8 The off-plane force as a function of filament orientation on the surface. The force is maximum for preferential anchoring $\psi_o = 90°$. ∅ indicates the diameter of the curved surface where the filament is attached.

multi-layer tubular liposomes[16,40] suggest that each FtsZ monomer should create a radial force in the range of 50 pN, which is within the values attainable if the filaments are properly oriented.

Previous estimates of the contractile force that can be exerted by the filaments are based either on filament bending or on filament sliding due to lateral interactions. The quantitative estimates are however strongly dependent on the filament properties considered. If filaments are considered to have a persistence length of 180 nm, they are too soft to exert enough force through curvature.[41] The authors then consider a lattice model to describe filament condensation on a flat surface and argue that a condensation transition from a low density state to a high-density state can generate a sufficient contractile force to achieve division. On the other hand, if the stiffness of the filaments is taken to be similar to that of actin, persistence length of ≈ 15 μm, much longer than any estimation done for FtsZ filaments,[11] a force generation mechanism based on a curvature change can be proposed.

The model presented here makes a quantitative estimate of filament properties using results from MD simulations. It indicates that the presence of torsion and curvature, combined with the attachment to the membrane surface, provides a strategy to modulate bending rigidity and a mechanism, different from GTP hydrolysis, to produce a switch from straight to curved conformation with respect to the membrane surface. The filament would behave as having two springs in series, a soft one due to the twist and a more rigid one due to the bending. If the soft twist is cancelled, the filaments become stiff and their orientation defines the filament surface morphology and also the stress generated on the surface.

The information available about the orientation and surface attachment of FtsZ to the membrane are both compatible with the suggestion that these elements could be regulated *in vivo* to trigger and modulate the force generation spatially and temporally within the cell. FtsZ is known to bind through its C-terminus end to the membrane through a flexible nonstructured region that is well conserved in many organisms.[35,36] Furthermore, FtsA and ZipA, the proteins that have been associated with FtsZ binding to the membrane, also contain a nonstructured region that can lie between FtsZ and the membrane.[42,43] In reconstituted systems, the distance and probably the stiffness of the membrane attachment of FtsZ through ZipA, modulated by the presence of charged lipids on the membrane, is indeed associated with the degree of curvature.[20] Furthermore, proteins that bundle FtsZ filaments like ZapA, ZapB and ZapC[44,45] could play a role similar to that of a strong surface attachment: inhibiting filament torsion and allowing the orientation and curvature of the filaments to prevail in determining the stiffness and stress transmitted to the membrane. Although the results obtained here refer only the analysis of single filaments, it would be worth exploring the role that bundling plays on the properties of the polymer fibers.[46]

Interestingly, very recent experiments using Polarized Fluorescence Microscopy have shown an unexpected disordered organization of the filaments.[47] It could well be that the disorder

detected could reflect the different monomer orientations due to torsion.

It is likely that lateral interactions and filament curvature both play important roles at different stages of the force generation process: lateral interactions between filaments could participate in condensing the filaments into a ring possibly exerting some force,[41,48] and filament curvature, once the twist is cancelled either through filament surface attachment or bundling, could produce the final power stroke. The quantitative evaluation provided by this model contributes to refine our picture of how FtsZ structure and surface binding come together to generate force on the underlying membrane.

Materials and methods

3D modelling and molecular dynamics

The three-dimensional model of the FtsZ pentamer in the presence of Mg^{++}-GTP and K^+ in the active centre was constructed by successive structural alignment of the two FtsZ subunits of the previously published MD-equilibrated FtsZ dimer,[24] essentially as described previously.[25] MD simulation was performed using the PMEMD module of the AMBER 12 package.[28] The modelled FtsZ polymer was surrounded by a rectilinear solvent box with a minimum distance of 15 Å from the edge of the box to the closest atom of the solute (the total number of atoms in the system: 288 517), and with periodic boundary conditions, using LEAP. As described previously[24,25] electrostatic interactions were represented using the smooth particle mesh Ewald methods with a grid spacing of 1 Å: K^+ ions were placed in a shell around the system using a coulombic potential in a grid of 1 Å as implemented in the XLEaP module of AMBER package. Adaptation to the AMBER force field ff99SB[27] was performed by 10 000 steps of energy minimization using a cut-off of 9 Å and a δt of 0.002 ps. During the initial heating phase (200 ps), the temperature was raised from 0 to 300 K, restraining the position of the Cα atoms with a force constant of 20 kcal mol^{-1}, reducing the force constant in a stepwise fashion in the subsequent phase. After equilibration, unrestrained MD was performed for 80 ns, relocating the hydrogen atoms using the SHAKE algorithm. As indicated in a previous work,[25] sufficient sampling for protein movements on the FtsZ modeled pentamer during MD trajectories was measured by calculation of the non-weighted covariance matrix of C-alpha atoms of the structure to obtain the cosine content (ci)[26] of the three first principal components. The results, far from a perfect cosine in all cases, indicated that the trajectories reached an overall sufficient sampling. The coordinates were saved for analysis of atom positions every 20 ps. Geometrical values were measured using *Cpptraj* (from AMBER 12 package). To illustrate that the trajectory had reached an overall sufficient sampling, the evolution of the cosine content calculated for the first principal component in a the whole 80 ns trajectory was measured (See Fig. S8†). A fast decrease of the cosine content was observed in the first 20 ns, providing an information about the convergence of the structure, far from random diffusion.[26]

Protein purification and assay

Mutation and overexpression of mut *E. coli* FtsZ S255C are explained in ref. 22 (see ESI† for further details). Expressed proteins were purified as described in ref. 21 except with the addition of 1 mM DTT in buffers to keep their cysteine residues in a reduced state. Protein purities were checked by SDS-PAGE and were found to be 98%. Protein concentrations were measured using the BCA assay (Pierce).

Preparation of S255C-EcFtsZ anchored to planar lipid bilayers

Separate 0.1 M stock solutions of the lipids dioleoyl phosphatidylcholine (DOPC), *E. coli* cardiolipin (ECCL) (Avanti Polar Lipids, Alabaster), or distearoyl *N*-(3-maleimido-1-oxopropyl)-L-phosphatidylethanolamine (DSPE-MAL) (NOF Corporation) were prepared in a $CHCl_3/CH_3OH$ 1/1 (v/v) solvent. A mixture of 90% DOPC (or ECPL)/10% DSPE-MAL or DOPC 80%/cardiolipin 10%/DSPE-Mal 10% mol mol^{-1} was evaporated under nitrogen and resuspended in Buffer L (50 mM Tris–HCl pH 7.4, 200 mM NaCl, 5 mM $CaCl_2$) at a final lipid concentration of 2.5 mM for preparing DOPC. To obtain Large Unilamellar Vesicles (LUVs) the suspension was extruded 31 times through a 200 nm pore membrane. To fuse the lipid bilayer on the substrate a diluted 0.1 mM solution of the LUVs was placed in contact with freshly cleaved mica for 45 min at 30 °C. Then, the samples were rinsed with Buffer Z (50 mM Tris–HCl pH 7.4, 500 mM KCl, 5 mM $MgCl_2$) to remove excess LUVs. In order to anchor each FtsZ mutant to the lipid bilayer surface, a 2 μM solution of the protein in buffer Z was incubated on the formed bilayer (ratio of 1 : 5 linker lipid head to protein) for several hours to ensure a complete coverage of the active surface. 100 μM TCEP was also added to reduce eventual disulfide bonds formed between proteins. After the incubation period the sample was rinsed with Buffer Z to remove excess protein.

AFM imaging

Atomic Force Microscopy (AFM) imaging was performed on the bilayer anchored FtsZ mutant in buffer after rinsing the excess protein in the presence of 5 mM GTP. AFM images were taken with a microscope from Nanotec Electrónica (Madrid, Spain) operated in the jump mode[23] in a liquid environment. The scanning piezo was calibrated using silicon calibrating gratings (NT-MDT, Moscow, Russia). Silicon nitride tips (Veeco) with a force constant of 0.05 Newton per m and 20 nm tip radius were used.

Acknowledgements

References

1 J. Mingorance, G. Rivas, M. Vélez, P. Gómez-Puertas and M. Vicente, Strong FtsZ is with the force:mechanisms to constrict bacteria, *Trends Microbiol.*, 2010, **18**, 348–356.

2 M. Vicente and A. I. Rico, The order of the ring: assembly of Escherichia coli cell division components, *Mol. Microbiol.*, 2006, **61**, 5–8.

3 M. Vicente, A. I. Rico, R. Martínez-Arteaga and J. Mingorance, Septum Enlightenment: Assembly of Bacterial Division Proteins, *J. Bacteriol.*, 2006, **188**, 19–27.

4 A. Mukherjee and J. Lutkenhaus, Dynamic assembly of FtsZ regulated by GTP hydrolysis, *EMBO J.*, 1998, **12**, 462–469.

5 D. Popp, M. Iwasa, H. P. Erickson, A. Narita, Y. Maéda and R. Robinson, Suprastructures and Dynamic Properties of Mycobacterium tuberculosis FtsZ, *J. Biol. Chem.*, 2010, **285**, 11281–11289.

6 S. Thanedar and W. Margolin, FtsZ Exhibits Rapid Movement and Oscillation Waves in Helix-like Patterns in Escherichia coli, *Curr. Biol.*, 2004, **14**, 1167–1173.

7 G. Fu, T. Huang, J. Buss, C. Coltharp, Z. Hensel and J. Xiao, In Vivo Structure of the E. coli FtsZ-ring Revealed by Photoactivated Localization Microscopy (PALM), *PLoS One*, 2010, **5**, e12680.

8 H. P. Erickson, Modeling the physics of FtsZ assembly and force generation, *Proc. Natl. Acad. Sci. U. S. A.*, 2009, **106**, 9238–9243.

9 J. F. Allard and E. N. Cytrynbaum, Force generation by a dynamic Z-ring in Escherichia coli cell division, *Proc. Natl. Acad. Sci. U. S. A.*, 2008, **106**, 145–150.

10 I. V. Surovtsev, J. J. Morgan and P. A. Lindahl, Kinetic Modeling of the Assembly, Dynamic Steady State, and Contraction of the FtsZ Ring in Prokaryotic Cytokinesis, *PLoS Comput. Biol.*, 2008, **4**, e1000102.

11 B. Ghosh and A. Sain, Origin of Contractile Force during Cell Division of Bacteria, *Phys. Rev. Lett.*, 2008, **101**, 178101.

12 C. Lu, M. Reedy and H. P. Erickson, Straight and Curved Conformations of FtsZ Are Regulated by GTP Hydrolysis, *J. Bacteriol.*, 2000, **182**, 164–170.

13 M. A. Oliva, S. C. Cordell and J. Löwe, Structural insights into FtsZ protofilament formation, *Nat. Struct. Mol. Biol.*, 2004, **11**, 1243–1250.

14 P. Mateos-Gil, A. Páez, I. Hörger, G. Rivas, M. Vicente, P. Tarazona and M. Vélez, Depolymerization dynamics of individual filaments of bacterial cytoskeletal protein FtsZ, *Proc. Natl. Acad. Sci. U. S. A.*, 2012, **109**, 8133–8138.

15 S. Pichoff and J. Lutkenhaus, Unique and overlapping roles for ZipA and FtsA in septal ring assembly in Escherichia coli, *EMBO J.*, 2002, **21**, 685–693.

16 M. Osawa, D. Anderson and H. P. Erickson, Reconstitution of Contractile FtsZ Rings in Liposomes, *Science*, 2008, **320**, 792–794.

17 M. Osawa, D. E. Anderson and H. P. Erickson, Curved FtsZ protofilaments generate bending forces on liposome membranes, *EMBO J.*, 2009, **28**, 3476–3484.

18 S. Arumugam, G. Chwastek, E. Fischer-Friedrich, C. Ehrig, I. Mönchand and P. Schwille, Surface Topology Engineering of Membranes for the Mechanical Investigation of the Tubulin Homologue FtsZ, *Angew. Chem., Int. Ed.*, 2012, **51**, 1185811862.

19 L. Hamon, D. Panda, P. Savarin, V. Joshi, J. Bernhard, E. Mucher, A. Mechulam, P. A. Curmi and D. Pastré, Mica Surface Promotes the Assembly of Cytoskeletal Proteins, *Langmuir*, 2009, **25**, 3331–3335.

20 P. Mateos-Gil, I. Márquez, P. López-Navajas, M. Jiménez, M. Vicente, J. Mingorance, G. Rivas and M. Vélez, FtsZ polymers bound to lipid bilayers through ZipA form dynamic two dimensional networks, *Biochim. Biophys. Acta*, 2012, **1818**, 806–813.

21 G. Rivas, A. López, J. Mingorance, M. J. Ferrándiz, S. Zorrilla, A. P. Minton, M. Vicente and J. M. Andreu, Magnesium-induced linear self-association of the FtsZ bacterial cell division protein monomer. The primary steps for FtsZ assembly, *J. Biol. Chem.*, 2000, **275**, 11740–11749.

22 M. Encinar, A. Kralicek, A. Martos, M. Krupka, A. Alonso, S. Cid, A. I. Rico, M. Jiménez and M. Vélez, Polymorphism of FtsZ filaments on lipid surfaces: role of monomer orientation, *Langmuir*, 2013, **29**, 9436–9446.

23 F. Moreno-Herrero, P. J. dePablo, R. Fernández-Sánchez, J. Colchero, J. Gómez-Herrero and A. M. Baró, Scanning force microscopy jumping and tapping modes in liquids, *Appl. Phys. Lett.*, 2002, **1**, 2620–2622.

24 J. Mendieta, A. I. Rico, E. López-Viñas, M. Vicente, J. Mingorance and P. Gómez-Puertas, Structural and Functional Model for Ionic (K+/Na+)and pH Dependence of GTPase Activity and Polymerization of FtsZ, the Prokaryotic Ortholog of Tubulin, *J. Mol. Biol.*, 2009, **390**, 17–25.

25 F. Martín-García, E. Salvarelli, J. I. Mendieta-Moreno, M. Vicente, J. Mingorance, J. Mendieta and P. Gómez-Puertas, Molecular dynamics simulation of GTPase activity in polymers of the cell division protein FtsZ, *FEBS Lett.*, 2012, **586**, 1236–1239.

26 B. Hess, Convergence of sampling in protein simulations, *Phys. Rev. E: Stat., Nonlinear, Soft Matter Phys.*, 2002, **65**, 031910–031910.

27 V. Hornak, R. Abel, A. Okur, B. Strockbine, A. Roitberg and C. Simmerling, Comparison of multiple Amber force fields and development of improved protein backbone parameters, *Proteins: Struct., Funct., Genet.*, 2006, **65**, 712–725, DOI: 10.1002/prot.21123.

28 D. A. Case, T. E. Cheatham, 3rd, T. Darden, H. Gohlke, R. Luo, K. M. Merz, Jr, A. Onufriev, C. Simmerling, B. Wang and R. J. Woods, The Amber biomolecular simulation programs, *J. Comput. Chem.*, 2005, **26**, 1668.

29 I. Hörger, E. Velasco, J. Mingorance, G. Rivas, P. Tarazona and M. Vélez, Langevin computer simulations of bacterial

protein filaments and the force-generating mechanism during cell division, *Phys. Rev. E: Stat., Nonlinear, Soft Matter Phys.*, 2008, **77**, 011902.

30 D. J. Turner, I. Portman, T. R. Dafforn, A. Rodger, D. I. Roper, C. J. Smith and M. S. Turner, The Mechanics of FtsZ Fibers, *Biophys. J.*, 2012, **102**, 731–738.

31 A. Dajkovic, G. Lan, S. X. Sun, D. Wirtz and J. Lutkenhaus, MinC Spatially Controls Bacterial Cytokinesis by Antagonizing the Scaffolding Function of FtsZ, *Curr. Biol.*, 2008, **18**, 235244.

32 J. Mingorance, M. Tadros, M. Vicente, J. M. Gonzz, G. Rivas and M. Vz, Visualization of Single Escherichia coli FtsZ Filament Dynamics with Atomic Force Microscopy, *J. Biol. Chem.*, 2005, **280**, 20909–20914.

33 J. M. González, M. Vélez, M. Jiménez, C. Alfonso, P. Schuck, J. Mingorance, M. Vicente, A. P. Minton and G. Rivas, Cooperative behavior of Escherichia coli cell-division protein FtsZ assembly involves the preferential cyclization of long single-stranded fibrils, *Proc. Natl. Acad. Sci. U. S. A.*, 2005, **102**, 1895–1900.

34 Y. Chen and H. P. Erickson, Conformational Changes of FtsZ Reported by Tryptophan Mutants, *Biochemistry*, 2011, **50**, 4675–4684.

35 A. J. Martín-Galiano, R. M. Buey, M. Cabezas and J. M. Andreu, Mapping Flexibility and the Assembly Switch of Cell Division Protein FtsZ by Computational and Mutational Approaches, *J. Biol. Chem.*, 2010, **285**, 22554–22565.

36 K. A. J. A. Gardner, D. A. Moore and H. P. Erickson, The C-terminal linker of Escherichia coli FtsZ functions as an intrinsically disordered peptide, *Mol. Microbiol.*, 2013, **89**, 264–275.

37 S. S. Andrews and A. P. Arkin, A Mechanical Explanation for Cytoskeletal Rings and Helices in Bacteria, *Biophys. J.*, 2007, **93**, 1872–1884.

38 I. Hörger, E. Velasco, G. Rivas, M. Vélez and P. Tarazona, FtsZ Bacterial Cytoskeletal Polymers on Curved Surfaces: The Importance of Lateral Interactions, *Biophys. J.*, 2008, **94**, L81–L83.

39 J. Hsin, A. Gopinathanand and K. C. Huang, Nucleotide-dependent conformations of FtsZ dimers and force generation observed through molecular dynamics simulations, *Proc. Natl. Acad. Sci. U. S. A.*, 2012, **109**, 9432–9437.

40 I. Hörger, F. Campelo, A. Hernez-Machado and P. Tarazona, Constricting force of filamentary protein rings evaluated from experimental results, *Phys. Rev. E: Stat., Nonlinear, Soft Matter Phys.*, 2010, **81**, 031922–031931.

41 G. Lan, B. R. Daniels, T. M. Dobrowsky, D. Wirtzand and S. X. Sun, Condensation of FtsZ filaments can drive bacterial cell division, *Proc. Natl. Acad. Sci. U. S. A.*, 2009, **106**, 121–126.

42 T. Ohashi, C. A. Hale, P. A. J. de Boer and H. P. Erickson, Structural Evidence that the P/Q Domain of ZipA Is an Unstructured, Flexible Tether between the Membrane and the C-Terminal FtsZ-Binding Domain, *J. Bacteriol.*, 2002, **184**(15), 4313–4315.

43 P. Szwedziak, Q. Wang, S. M. V. Freund and J. Lowe, FtsA forms actin-like protofilaments, *EMBO J.*, 2012, **31**(10), 2249–2260.

44 E. Galli and K. Gerdes, FtsZ-ZapA-ZapB Interactome of Escherichia coli, *J. Bacteriol.*, 2012, **194**, 292–302.

45 C. A. Hale, D. Shiomi, B. Liu, T. G. Bernhardt, W. Margolin, H. Niki and P. A. J. de Boer, Identification of Escherichia coli ZapC (YcbW) as a Component of the Division Apparatus That Binds and Bundles FtsZ Polymers, *J. Bacteriol.*, 2011, **193**, 1393–1404.

46 A. Dajkovic, S. Pichoff, J. Lutkenhaus and D. Wirtz, Cross-linking FtsZ polymers into coherent Z rings, *Mol. Microbiol.*, 2010, **78**, 651668.

47 F. Si, K. Busiek, W. Margolin and S. X. Sun, Organization of FtsZ Filaments in the Bacterial Division Ring Measured from Polarized Fluorescence Microscopy, *Biophys. J.*, 2013, **105**, 19761986.

48 A. Páez, P. Mateos-Gil, I. Hörger, J. Mingorance, G. Rivas, M. Vicente, M. Vélez and P. Tarazona, Simple modeling of FtsZ polymers on flat and curved surfaces: correlation with experimental in vitro observations, *PMC Biophys.*, 2009, **2**, 8.